Cloud Image Processing and Analysis Based Flatfoot Classification Method

Ming-Shen Jian, Jun-Hong Shen, Yu-Chih Chen,
Chao-Chun Chang, Yi-Chi Fang, Ci-Cheng Chen, Wei-Han Chen

***Abstract*—**In this paper, the Cloud Image Processing and Analysis based Flatfoot Classification method that help doctors determine the flat feet is proposed. Via using image processing and analysis established on different virtual machines on cloud, the proposed method can remove noise and shape the images of the foot based on X-ray picture. The individual X-ray image after image processing is divided into four blocks according to the proposed division method which considering the percentage of each foot. By dividing the original image into four individual sub-partition of image, each divided image can be delivered to different analysis algorithms for key-point finding. Each image can be processed based on individual virtual machine on cloud. According to the proposed algorithms implemented on cloud for individual sub-partition of original image, the system can find four decision points of each block. Based on the integration of processing results from different algorithms, the system can automatically identify flat feet. Furthermore, the information and identification results can be provided to the doctor for further manual identification. In addition, the decision point can be also manually selected. In other words, according to the selection made by the doctor, the system can make the results more accurately and objectively. The simulation presents that the accuracy can be enhanced based on the dpi of the X-ray picture. Moreover, different methods used for decision points finding provide different performance.

***Keywords*—** Cloud, Edge Detection, Flatfoot, Medical Image Processing.

Ming-Shen Jian is with the Department of Computer Science and Information Engineering, National Formosa University, Huwei, Yunlin, Taiwan, R.O.C. (e-mail: jianms@nfu.edu.tw).

Jun-Hong Shen is with Department of Information Communication, Asia University, Wufeng, Taichung, Taiwan, R.O.C. (corresponding author) (phone: 886-4-23323456ext.20006; fax: 886-4-23305824; e-mail: shenjh@asia.edu.tw).

Yu-Chih Chen is with the Department of Computer Science and Information Engineering, National Formosa University, Huwei, Yunlin, Taiwan, R.O.C. (e-mail: himaboy826@gmail.com).

Chao-Chun Chang is with the Department of Computer Science and Information Engineering, National Formosa University, Huwei, Yunlin, Taiwan, R.O.C. (e-mail: wert943@gmail.com).

Yi-Chi Fang is with the Department of Computer Science and Information Engineering, National Formosa University, Huwei, Yunlin, Taiwan, R.O.C. (e-mail: ken801227@gmail.com).

Ci-Cheng Chen is with the Department of Computer Science and Information Engineering, National Formosa University, Huwei, Yunlin, Taiwan, R.O.C. (e-mail: q462246@gmail.com).

Wei-Han Chen is with the Department of Computer Science and Information Engineering, National Formosa University, Huwei, Yunlin, Taiwan, R.O.C. (e-mail: k0937404150@gmail.com).

I. Introduction

A. Background and Motivation

With advances in technology, medical instrumentation and techniques are constantly improved. The medical image provided doctors a basis for illness detection. Since Rontgen discovered the X-ray, the demand on using X-ray to determine disease increases such as medical examination for military service.

Currently, medical examination for military service such as flatfoot based on X-ray images becomes the main basis. However, such a huge number of medical images will result in the doctor's heavy burden. Therefore, via using an intelligent recognition system automatic analysis, doctors will be able to reduce the burden greatly. In addition, according to the consistent system in analyzing the images, the ratio of wrong identification for flatfoot can be reduced.

Therefore, in this paper, we propose the flatfoot automatic classification method based on image recognition and analysis that includes image processing methods for the foot X-ray image, flatfoot determining algorithm, and measurement data providing.

1) Detection of flatfoot

Flatfoot detection is often used in the military service medical examination and customized footwear. Because of the lack of a normal arch, walking and jogging will make foot more pressure, [3]. Those methods used to determine the flatfoot contains the following three ways:

a. By the arch

The arches of the foot are formed by the tarsal and metatarsal bones. The arch of flatfoot is too low. However, this method is detected by doctor's experience, with no real basis. Fig.1 shows the difference of normal and flat arch.

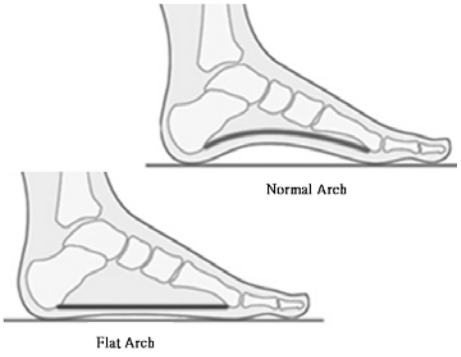

Fig. 1 Difference of normal and flat arches

b. By the arch angle

Medial aspect of the foot based on X-ray image can find two lines. The first line can obtained by connect both ends of the lower edge of the fifth metatarsal. The connection according to the lower edge of the calcaneus ends can be obtained as the second line. Then, the intersection angle of the two lines is called arch angle shown as Fig.2. If the angle "α" is greater than 165∘, we called flatfoot.

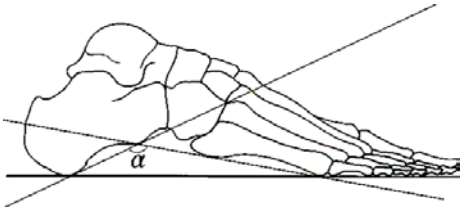

Fig. 2 Arch angle
Source : Conscription Agency, Taiwan
(http://www.nca.gov.tw/)

c. By the footprint

This method detects the lengths of "arch empty" and "middle foot" on footprint. As Fig.3, it is called a normal foot if the length of arch empty and middle foot was similar; in opposition, it is called a flatfoot if the arch empty less than 1 cm which is significantly different from middle foot.

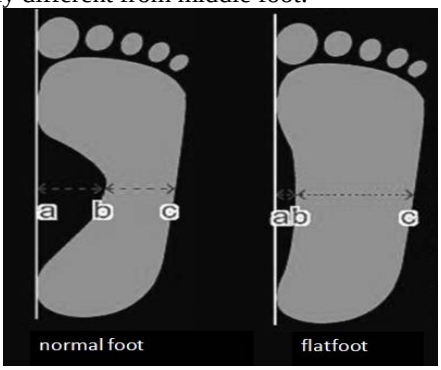

Fig. 3 Detect by the footprint

Detection according to the arch is difficult by single picture, because that the information is so few and difficult to be transformed as data. Furthermore, detection according to the footprint may have cause errors due to human factors. Therefore, this paper employs the method that detect by the arch angle.

2) Noise reduction

The main noise in the medicine X-ray image is quantum mottle. The noise is usually associated with X-ray radiation intensity as well as artificial noise relate.

In digital radiography, the sampling pitch of grid density and raster direction will affect the noise size in image. If the radiations cause moire, the noise of image increases. Therefore, the X-ray images must reduce these noises in order to the accurate diagnosis.

In order to reduce the film graininess of image, X-ray irradiation intensity must be increased with detrimental to the patient. However, when the noise is too much, through the edges detection is not suitable, because the information of the edges will lose. On the other hand, to use the band-pass filter or a low pass filter for the grid method reducing may have a chance to produce relatively poor quality images. Therefore, the filter must be carefully selected [6,7].

This paper compares three common filters: Mean filter, Median filter, and Gaussian Filter. Because that mean filter will cause the edge fuzzy; median filter is not inappropriate to process Gaussian noise, the Gaussian filter is selected and used to reduce noise.

3) Edge detection

To detect the flatfoot, we need to find foot bones edge information first. The following three guidelines can be used to decide the quality of the edge detection methods shown as follows:

a. Detection: The important edge line cannot be lost. In addition, there should be no forged reaction. In other words, to find out all gray-changed edges and remove noise at the same time, to make the signal to noise ratio increasing becomes an important issue.

b. Localization: The distance between the real position of gray-changed edge and that found by detector is as small as possible. The less distance will provide the higher positioning accuracy.

c. One response: Compressing the multi-sensing data as a single edge. Some edge detector will perceive one edge as multiple edges. Therefore, the system must determine a proper data from multi-sensing data.

The traditional edge detection methods usually only meet the first two criteria with the edges extracted errors and noise [1,8]. Canny added a restraint condition to make the edge detector not only have a good ability to detect and locate, but also find a more correct edge. Furthermore, there will not be too thick edge problem. Therefore, this paper uses Canny edge detection to detect foot for characteristic information.

4) Cloud

To obtain the higher performance of image processing, many applications provide the cloud based services for system users with less cost of hardware and infrastructure. In addition, many algorithms or processing methods can be repeatedly and rapidly used for different users. The computing performance of cloud is better than the normal personal computer.

The cloud service infrastructure can be divided into three levels [13, 14]: Infrastructure as a Service, Platform as a Service, and Software as a Service. Different processing methods can be independently implemented based on different virtual machines on cloud as services. By using the virtual implementation of hardware and operating systems, cloud computing provides users the ability to create or deploy their own applications with huge computing resources. Many services (Christensen, 2009) including Amazon's EC2, IBM's Smart Business cloud offerings, Microsoft's Azure, and Google's AppEngine are based on cloud computing. According to the structure of cloud computing, users' application can be established individually on virtual machines. Cloud users can access the services via Internet connection.

II. Literature Review

A. Gaussian Blur

Gaussian blur is a linear smoothing filter used to eliminating Gaussian noise. It is widely used in image processing to reduce noise in the process [9,10,15]. Gaussian blur is an algorithm used to weighted average the whole image. Each pixel value is produced by weighted average calculation of itself and neighboring pixels. Fig.4 is the comparison of original image and Gaussian blur.

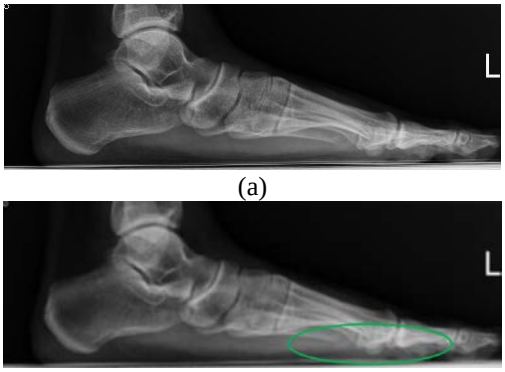

(a)

(b)

Fig. 4 Comparison of the original image and the image processed by the Gaussian blur: (a) the original image, (b) the image processed by the Gaussian blur.

The one-dimensional calculation is shown in Eq.(1), and the two-dimensional calculation is shown in Eq.(2), where σ is the standard deviation of the normal distribution.

$$G(x) = \frac{1}{\sqrt{2\pi}\sigma} e^{-\frac{x^2}{2\sigma^2}} \quad (1)$$

$$G(x, y) = \frac{1}{2\pi\sigma^2} e^{-\frac{x^2+y^2}{2\sigma^2}} \quad (2)$$

Gaussian blur which uses a mask scans each pixel in image. It calculates the weighted average of neighboring pixels to replace the center pixel value. The mask size is usually 3*3 or 5*5 (σ = 1). An example is shown in Fig. 5.

$$\frac{1}{16} \times \begin{bmatrix} 1 & 2 & 1 \\ 2 & 4 & 2 \\ 1 & 2 & 1 \end{bmatrix} \qquad \frac{1}{273} \times \begin{bmatrix} 1 & 4 & 7 & 4 & 1 \\ 4 & 16 & 26 & 16 & 4 \\ 7 & 26 & 41 & 26 & 7 \\ 4 & 16 & 26 & 16 & 4 \\ 1 & 4 & 7 & 4 & 1 \end{bmatrix}$$

Fig. 5 Gaussian blur 3*3 and 5*5 mask

When processing images with this mask, the overall image gray distribution features can be kept more completely. In this paper, the 3 * 3 mask is used.

B. Canny edge detection

Canny edge detection method becomes a standard edge detection method and developed by John Canny from 1986. The parameters can be adjusted according to different requirements to identify different edge characteristics [2,16]. Fig. 6 is the processes of the Canny edge detection method.

Since Canny edge detection method can minimize errors and improve the signal to noise ratio during the edge identifying, the edge detected according to the method can be close to the real edge.

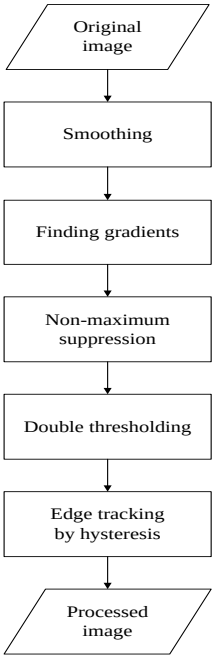

Fig. 6 The flowchart of Canny edge detection

A real edge should not be detected more than once. Therefore, in very complex image information, the Canny edge detection method can be used to deal with the complex image for the features Information. Fig. 7 is the comparison of original image and the image after the Canny edge detection.

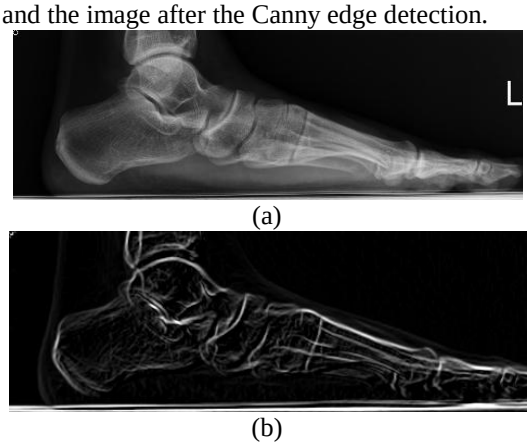

(a)

(b)

Fig. 7 Comparison of the original image and the image processed by the Canny edge detection: (a) the original image, (b) the image process by the Canny edge detection.

The operations of the Canny edge detection are given as follows:

1) Smoothing: To prevent that the edges of an error is detected, the system or method must reduce the noise. The smoothing filter often used which includes low-pass filter, median filter, mean filter, Gaussian blur, etc.

2) Finding gradients: Canny algorithm can find the maximum change grayscale edge. It also calculates each pixel gradient value of the image by Sobel operator and divides into the

x-direction (Gx) and *y*-direction (Gy) as (3). Gradient strength, also known as the edge strength, can be evaluated by Euclidean distance measure as (4) or the Manhattan distance measure as (5).

$$K_{G_x}=\begin{bmatrix}-1 & 0 & 1\\ -2 & 0 & 2\\ -1 & 0 & 1\end{bmatrix}, K_{G_y}=\begin{bmatrix}1 & 2 & 1\\ 0 & 0 & 0\\ -1 & -2 & -1\end{bmatrix} \quad (3)$$

$$|G|=\sqrt{G_x^2+G_y^2} \quad (4)$$

$$|G|=|G_x|+|G_y| \quad (5)$$

In order to be able to determine the location of the edge precisely, the edge gradient direction must be determined according to (6).

$$\theta=\tan^{-1}\left(\frac{|G_y|}{|G_x|}\right) \quad (6)$$

3) Non-maximum suppression: The purpose of this step is to sharpen edge gradient of the image. The maximum gradient in the image area should be retained, and the non-maximal gradient value edge should be removed. Each gradient value is evaluated according to eight-connected neighbor. The gradient direction can be simplified into four regions. At last, the local maximum value can be decided. Fig. 8 is the schematic diagram of gradient direction.

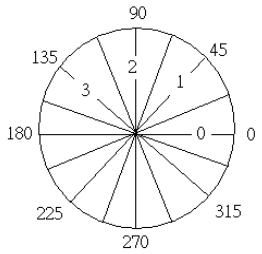

Fig. 8 Schematic diagram of gradient direction

4) Double thresholding : Those remaining pixel after the previous step may be true edges, noises, or color change. The Canny edge detection can use double threshold, T_{high} and T_{low}, to separate. The pixel higher than T_{high} is marked as strong; the pixel lower than T_{low} was removed; the pixel between two thresholds is marked as weak. By this way, the system can ensure that unwanted noise will not affect the results of edge detection.

5) Edge tracking by hysteresis: After double-threshold classification, strong edge can be immediately marked as the final edge of the image. If the weak edge is adjacent to the strong edge, it may be the true edge. Otherwise, it may be noise. Because weak edge may be true edge and connected with the strong edges directly, edge tracking can use eight-connected and binary large object to analyze. At least one strong edge points will be retained.

III. FLATFOOT AUTOMATIC CLASSIFICATION METHOD

In this paper, in order to effectively distinguish flatfoot, the proposed system combines Gaussian blur and Canny edge detection for image processing. The proposed system also includes three new algorithms to compute the feature point. According to the proposed three algorithms, the proposed system can achieve the function of automatic classification for flatfoot, and provide the physician the reference and basis information. Fig. 9 is the system flow chart.

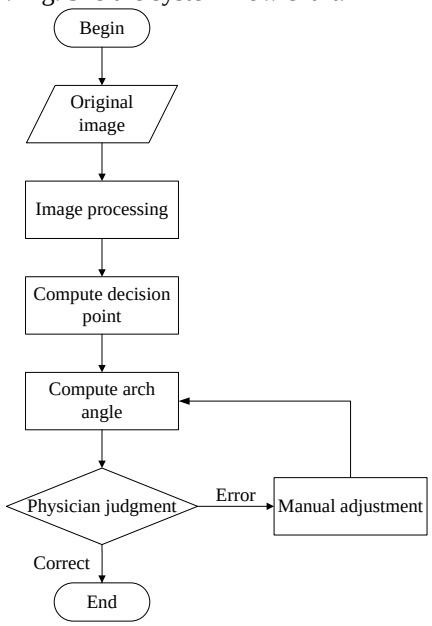

Fig.9 System flowchart

A. *Image processing*

First, image is proportionally reduced to less than 500 * 500 pixels. Then, the Gaussian blur is used to reduce noise. At last, the Canny edge detection is adopted to find out foot bones edge information shown in Fig.10. Fig.11 shows the pre-process flow.

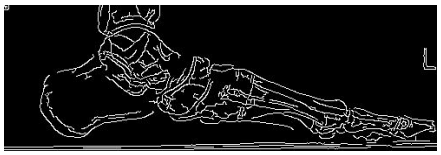

Fig. 10 Edge image

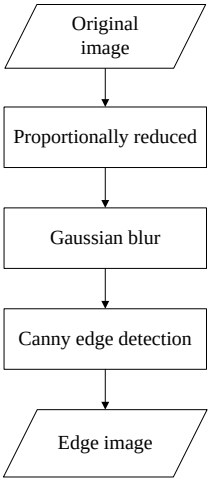

Fig. 11 Pre-process flowchart

B. Area segmentation

Four decision points are located at the ends of the fifth metatarsal and the ends of the calcaneus. In this paper, the image is split into four areas shown in Fig.12.

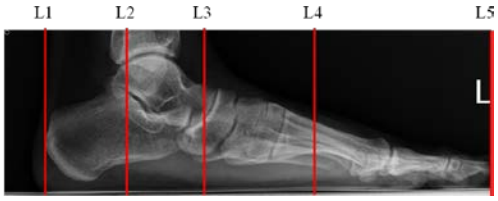

Fig. 12 Four areas

The locations of different lines (L_1 to L_4) are based on a certain percentage of the average person's foot bones. The lower edge of the foot bones is shown in Fig.13.

Fig. 13 Lower edge

When an individual user starts to use the proposed system, the system requests the client user to upload the X-ray image. Each image will be segmented according to the certain percentage of the average person's foot bones. Then, the original image can be divided into four sub-image area.

When the server in cloud receives the processing request from the client application, the main program (also called JobTracker depicted in Fig. 14) will handle the processing request according to the dividing results based on the area segmentation. Then, the data and partial image related to the original X-ray image should be delivered to the corresponding sub-server (also called TaskTracker) for the further processing based on the corresponding decision point selection method. Finally, the decision points of different partial images can be evaluated and selected.

Since different decision points can be found based on different selection algorithms, the algorithm for decision point finding can be executed independently. In other words, each decision point finding procedure or method is implemented independently as the individual cloud procedure based on virtual machines.

After selecting decision points in each individual Tasktracker, the Jobtracker integrates the selection results from different virtual machines based on cloud. At last, the decision of the flatfoot can be provided by the Jobtracker.

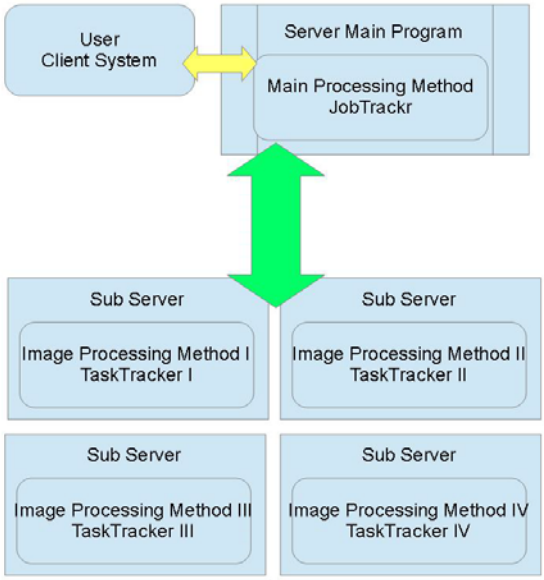

Fig. 14 Processing in the cloud system

C. Finding decision points

According to Fig.12, there are four areas between different lines called L_{12}, L_{23}, L_{34}, and L_{45}. In this paper, to identify each decision point, three algorithms are proposed as follows:

1) The first area and the third area (L_{12} and L_{34}): The decision points in these two areas are: one is at the left endpoint of calcaneus, and another is at the left endpoint of fifth metatarsal. In these two areas, we use the (7) to select the decision points. P_{j_x} is the *x* coordinate of P_j, $P_{j_{l_x}}$ is the *x* coordinate of the point that distance N unit pixels before P_j. P_{j_y} is the *y* coordinate of P_j, $P_{j_{l_y}}$ is the *y* coordinate of the point that distance N unit pixels before P_j. $P_{j_{r_x}}$ is the *x* coordinate of the point that distance N unit pixels after P_j. $P_{j_{r_y}}$ is the *y* coordinate of the point that distance N unit pixels after P_j. Then, the P_j with the minimized value, C_j, indicates the most turning point on this line from P_1 to P_2. In other words, it will be selected as the decision point.

$$C_j = \min(\pi - \tan^{-1}(\frac{P_{j_y} - P_{j_{l_y}}}{P_{j_x} - P_{j_{l_x}}}) + \tan^{-1}(\frac{P_{j_{r_y}} - P_{j_y}}{P_{j_{r_x}} - P_{j_x}})) \quad (7)$$

In this paper, the shape of the lower edge of bones in these two areas can be approximated to Fig.15. We assume that P_1 is the most left pixel of the lower edge; P_2 is the most right pixel. P_j indicates each pixel between P_1 and P_2. P_{jl} and P_{jr} are two points before or after the P_j with *n* pixels distance.

We assume L_1 is the connection between P_j and P_{jl}, and L_2 is the connection between P_j and P_{jr}. According to , each P_j will get a value. P_j with the minimum value is called the decision point.

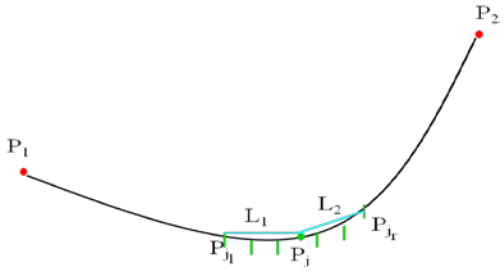

(a)

(b)

Fig. 15 (a)The shape of lower edge of bones in first area and (b) the result of decision point searching.

2) The second area (L_{23}): The decision point in this area is the right endpoint (most right point) of calcaneus. We use (8) to find and select the decision point. M_1 is the slope of L_3; M_2 is the slope of L_4. There have n_1 pixel in L_3 and n_2 pixel in L_4. P_{h_x} is the X coordinate of P_h, k_x is the X coordinate of k. P_{h_y} is the Y coordinate of P_h, N is the set of coordinates of P_3 to P_4.

$$\min\Big(\sum_{k=1}^{n_1} | M_1(k_x - P_{h_x}) + P_{h_y} - N_{k_y} | + \sum_{m=1}^{n_2} | M_2(m_x - P_{h_x}) + P_{h_y} - N_{m_y} |\Big) \quad (8)$$

The shape of the lower edge of the bone in this area is shown as Fig. 16. In this paper, we assume that P_1 is the most left pixel of the lower edge; P_2 is the most right pixel. P_j indicates pixel between P_1 and P_2. First, every P_j connect P_1 and P_2 respectively (L_1 and L_2). According to (8), after calculating each P_j, the P_j with minimum value is called the decision point.

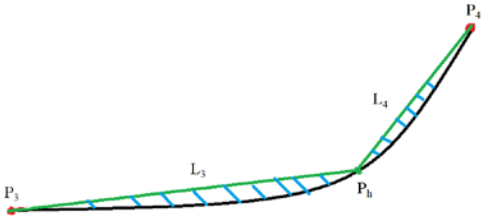

(a)

(b)

Fig. 16 (a) The shape of lower edge of bones in second area, (b) the result of decision point searching

3) The fourth area (L_{45}): The decision point in this area is the right endpoint of fifth metatarsal. The shape of the lower edge of the bone in this area is shown in Fig.17.

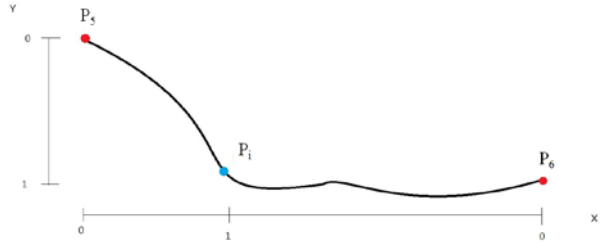

(a)

Fig. 17 (a) The shape of lower edge of bones in fourth area, (b) the result of decision point searching

In this paper, we assume P_1 is the most left pixel of the lower edge; P_2 is the most right pixel. And P_j indicates each pixel between P_1 and P_2. This region has many and complex number of bones with the image information cluttered Therefore the system must define a degree value (0 to 1) in the X-axis and Y-axis respectively based on (9). Then, P_j with maximum value is called the decision point. X_{p_j} is the degree value of P_j on the X-axis; Y_{p_j} is the degree value of P_j on the Y-axis. Then, the difference between different P_j can be evaluated obviously according to (9).

$$X_{p_j}{}^2 + Y_{p_j}{}^2 \quad (9)$$

Through the above algorithm, the proposed system and system users can find the decision point and calculate the angle of arch. If decision points are discovered by the system with the expectations missing, system user can manually select the

correct position themselves. The system will recalculate and generate a new value.

IV. System and Results

A. System interface

For convenience, user can import the images in a folder, and operating in a simple interface. The system will automatically find the decision points and shows the angle value on the interface. Then through the physician determine correctness, if errors, physicians can direct give a new decision point on the user interface, and the system will recalculate the angle value. To facilitate the recognition click position, the system marks the position of the mouse pointer by a vertical line. The user interface is show as Fig. 18.

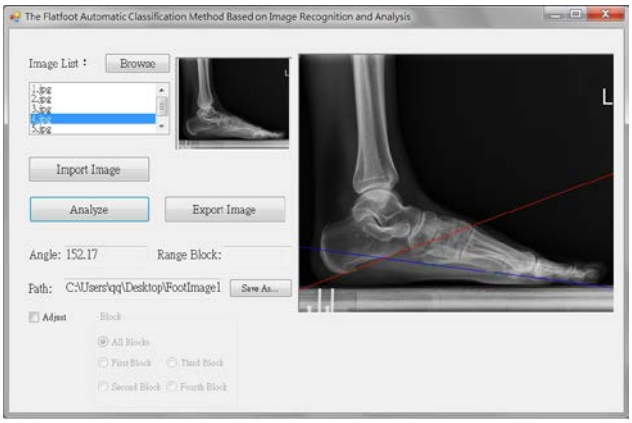

Fig.18 User interface

B. Research results

In this study, four random selected images shown in Fig. 19 are tested for statistical analysis. In the beginning, the original X-ray image will be edge imaged. Then, lower edge is used for the X-ray image. These six images do the Gaussian blur degradation from 0 to 90 percent, and calculate the angle value every 10 percent, as shown in Fig. 20. According to Fig. 20, the angle value of most images calculated by this system will not change much, no matter how much the degree of degradation is.

(a)

(b)

(c)

(d)

(e)

(f)

Fig. 19 The six original images for statistical analysis.(a) - (f) are Image 1 - Image 6

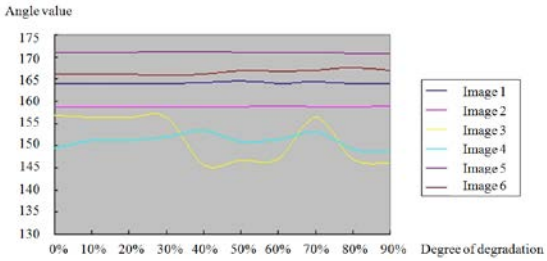

Fig. 19 Comparison of the degree of degradation

Due to that four decision points are located at the ends of the fifth metatarsal and the ends of the calcaneus, according to the percentage of the foot, the original images are divided into four partial areas. Based on the proposed system, each partial area is sent to the corresponding sub-server (TaskTracker with different image processing methods) for decision point finding. To increase the performance and reduce the time delay, the image analysis and processing is implemented based on OpenCV.

The decision points searching result of the four areas is shown in Fig. 21. There are four areas divided from the original X-ray image according to the percentage of the original foot.

Each partition area is processing by different algorithms based on individual virtual machine. Therefore, after processing, the JobTracker (main program) integrates the four partial areas processed by TaskTrackers (sub-server) with different proposed image processing algorithms. Each decision point is searched and found according to corresponding algorithm.

Fig. 21 The integration result of four areas after image processing

Based on the integration result of these four areas, the proposed system create two lines according to the decision points, as shown in Fig. 22. The first line is created based on the decision points from the first and second area. The second line is created according to the decision points from the third and fourth area. According to the created lines, the angle of these two lines can be evaluated. In other words, the foot can be classified as the flatfoot or not according to the angle.

Fig. 22 The angle of two lines according to four decision points

V. Conclusion

This paper uses an automatic classification method to determine the flatfoot from X-ray images. This method adopts Gaussian Blur and Canny edge detection based on OpenCV to identify foot bones edge information. Through the algorithm proposed by this paper, the decision point defined in this paper can be identified. Furthermore, based on cloud computing, the computing load can be distributed into different virtual machines. The proposed system can integrated the processing results for flatfoot classification.

The computing results of the proposed method show the good performance of most case. This paper presents the following contributions:

1) Doctor can improve the accuracy of judgment. And significantly improve the convenience of judgment in medical examination for military service.
2) Proposed three algorithms to compute the decision point.
3) Provides the interface to make the operation more convenient.

To increase the accuracy of identification, the proposed method needs a lot of foot X-ray images for testing and system learning. In the future, we hope to cooperate with domestic medical university to get more samples, and improve the system according to doctor's reference.

ACKNOWLEDGMENT

This research was supported in part by Asia University under grant no. 102-asia-51.

REFERENCES

[1] H. Moon, R. Chellappa, and A. Rosenfeld, "Optimal edge-based shape detection," *IEEE Trans. on Image Processing*, Vol.11, No.11, pp. 1209–1227, November 2002.
[2] J. Canny, "A computational approach to edge detection," *IEEE Trans. On Pattern Analysis and Machine Intelligence*, Vol.PAMI-8, No. 6, pp. 679–698, November 1986.
[3] P.Y. Chou, Y.Y. Chen, C.H. Liao, X.Y. Guan, S.C. Li, W.K. Wu, and H.C. Lo, "The influence of different imaging postures on flatfoot evaluation," *Chinese Journal of Radiologic Technology*, Vo.33, No.1, pp. 63-68, Jun 2009.
[4] M. Fakheri, T. Sedghi, M.G. Shayesteh, and M.C Amirani, "Framework for Image Retrieval Using Machine Learning and Statistical Similarity Matching Techniques," *IET Image Processing*, Vo.7, No.1, pp. 1–11, February 2013.
[5] D.J. Michael, and A.C. Nelson, "HANDX: a model-based system for automatic segmentation of bones from digital hand radiographs," *IEEE Trans. on Medical Imaging*, Vol.8, No.1, pp. 64–69, August 2002.
[6] A. Leigh, A. Wong, D.A. Clausi, and P. Fieguth, "Comprehensive analysis on the effects of noise estimation strategies on image noise artifact suppression performance," in *Proc. of the 2011 IEEE International Symposium on Multimedia*, 2011, pp. 97–104.
[7] G. El Fakhri, S.C. Moore, P. Maksud, and M.F. Kijewski, "The effects of compensation for scatter, lead X-rays and high-energy contamination on lesion detectability and activity estimation in Ga-67 imaging," *IEEE Nuclear Science Symposium Conference Record*, Vol.3, pp. 1784–1786, November 2002.
[8] L. Duan, Y. Zhao, and Y. Xue, "Study on medical image edge extraction," in *Int. Conf. on Computer Science and Service System*, 2011, pp. 3589–3592.
[9] J. Ryu, and T.H. Nishimura, "Fast image blurring using lookup table for real time feature extraction," in *IEEE Int. Symp. on Industrial Electronics*, 2009, pp. 1864–1869.
[10] E.S. Gedraite, and M. Hadad, "Investigation on the effect of a gaussian blur in image filtering and segmentation," in *Proc. of ELMAR*, 2011, pp. 393–396.
[11] H. Kwon, S.Z. Der, and N.M. Nasrabadi, "An adaptive segmentation algorithm using iterative local feature extraction for hyperspectral imagery," in *Proc. of Int. Conf. on Image Processing*, 2001, pp. 74–77.
[12] S. Mahmoodi, B.S. Sharif, E.G. Chester, and J.P. Owen, "Automated vision system for skeletal age assessment using knowledge based techniques," in *Proc. of Sixth Int. Conf. on Image Processing and Its Applications*, 1997, pp. 809–813.
[13] F. Garcia-Sanchez, E. Fernandez-Breis, R. Valencia-Garcia, E. Jimenez, J.M. Gomez, J. Torres-Nino, D. Martinez-Maqueda, "Adding Semantics to Software-as-a-Service and Cloud Computing," *WSEAS Trans. on Computers*, Vol. 9, No. 1, pp. 154-163, January 2010.
[14] J. Rietz, R. Macedo, C. Alves, J.V.D. Carvalho, "Efficient lower bounding procedures with application in the allocation of virtual machines to data centers," *WSEAS Trans. on Information Science & Applications*, Vol. 8, No. 1, pp. 157-170, January 2011.

[15] I.V. Gribkov, P.P. Koltsov, N.V. Kotovich, A.A. Kravchenko, A.S. Koutsaev, A.S. Osipov, and A.V. Zakharov, "Comparative study of image segmentation algorithms," in *Proc. of the 8th WSEAS Int. Conf. on Signal, Speech and Image Processing*, 2008, pp. 21-28.

[16] M.A. Osman, M.Y. Mohamad, and R. Abdullah, "Parallelizing an edge detection algorithm for image recognition to classify paddy and weeds leaf on sun fire cluster system," in *Proc. of the 7th WSEAS Int. Conf. on Software Engineering, Parallel and Distributed Systems*, 2008, pp. 56-60.